# TECHNICAL AND AERODYNAMICAL ASPECTS OF A HIGH PRESSURE SYNTHESIS GAS TURBOCOMPRESSOR MODERNIZATION

*W. Kryłłowicz – Z. Kozanecki – K. Kabalyk*
Lodz University of Technology, Institute of Turbomachinery, Lodz, Poland
kirill.kabalyk@p.lodz.pl
*P. Świder – Z. Kozanecki Jr*
Neo-Tec Sp. z. O. O., Plock, Poland

## ABSTRACT

**The article is devoted to the description of the modernization of a multihull process centrifugal compressor for synthesis gas. The main reason for the revamp was the desire to adapt the conventional machine (45 years of operation) for newer operational requirements: the decrease of compressor discharge pressure to the level of 140 bar from the level of 211 bar with the corresponding alteration of the mass flow rate.**

**The scheme accepted as a final modernization conception required the manufacturing of three completely new rotor and casing assemblies. Major design modifications concerned the impellers' geometry, introduction of vaneless diffusers and the abradable labyrinth seals. Most of the stages were "optimized" using the in-house semi-empirical 1D code and ANSYS CFX commercial code. The performance of a single optimized stage was tested experimentally. The paper reveals the main results of these measurements and their comparison to numerical simulations results. The start-up tests of the modernized assembly showed its almost 100% conformity to the requirements in the output and the efficiency rise of about 5%.**

**Key words:** centrifugal compressor modernization, low flow coefficient centrifugal impeller

## NOMENCLATURE

| | |
|---|---|
| b | meridional height of the compressor stage flow channel (m) |
| c | absolute flow velocity (m/s) |
| D | diameter (m) |
| HP | high pressure |
| IGV | inlet guide vanes |
| IT TUL | Institute of Turbomachinery, Lodz University of Technology |
| k | isentropic constant |
| LP | low pressure |
| LSD | low-solidity diffuser |
| $\dot{m}$ | mass flow rate (kg/s) |
| $M_u$ | specific Mach number (based on the impeller tip speed) [$= u_2 / \sqrt{kRT_{in}^*}$ ] |
| MP | medium pressure |
| $\Delta$p | pressure drop (Pa) |
| p | pressure (Pa) |
| PC | personal computer |
| R | gas constant (J/(kg*K)) |
| T | temperature (K) |
| $Tu$ | Turbulence intensity |
| u | tangential velocity (m/s) |
| $\dot{V}$ | volume flow rate ($m^3$/s) |
| VD | vaned diffuser |
| VLD | vaneless diffuser |

| | |
|---|---|
| z | blade number, stage number (Table 3) |
| $\alpha$ | blade (flow) angle in stationary frame of reference (deg.) |
| $\beta$ | blade (flow) angle in rotating frame of reference (deg.) |
| $\Phi$ | specific flow coefficient [$= 4\dot{m}/(\rho_{in}^{*}\pi D_2^2 u_2)$] |
| $\eta$ | efficiency [=useful polytropic (isentropic) energy/supplied energy] |
| $\nu$ | hub ratio [$= D_{\text{hub}} / D_2$] |
| $\Pi$ | pressure ratio of entire compressor [$= p_{\text{out}} / p_{\text{in}}$] |
| $\pi$ | pressure ratio of isolated stage [$= p_4 / p_0$] |
| $\rho$ | density (kg/m$^3$) |

**Subscripts**

| | |
|---|---|
| 0 | refers to stage inlet |
| 2 | refers to impeller outlet |
| 4 | refers to diffuser outlet |
| bl | blade |
| c | compressor |
| conv | converter |
| d | refers to design (nominal) operating condition |
| fr | friction |
| i | internal, current value |
| in | inlet |
| leak | leakage |
| op | opening |
| out | outlet |
| p | polytropic |
| r | refers to radial direction |
| rec | recirculation |
| s | isentropic |
| u | refers to circumferential direction |

**Superscripts**

| | |
|---|---|
| * | refers to total parameters |

## INTRODUCTION

The experience of modernization of process centrifugal compressors utilized among others in chemical industry has been in common practice within Polish enterprises over the last four decades. As a result, a vast amount of knowledge on typical issues and challenges concerning compression machinery modernization has been collected and was reported regularly in the forms of papers (Kryllowicz, 2007, 2011) and monographs (Kryllowicz, 2013, Kozanecki, 2008). This paper, represents the example of a complex revamp of a high-pressure multi-hull machine utilized in ammonia production process. The following sections are devoted to the description of the conventional machine design, steps of the modernization and its outcomes.

## CONVENTIONAL COMPRESSOR

A simplified design scheme of the original machine is shown in Fig. 1. The whole unit is comprised of three compression casings (marked as “low pressure” (LP), “medium pressure” (MP) and “high pressure” (HP)) and a steam turbine casing (not shown in Fig. 1). Each of the casings is designed in a so-called “barrel-type” fashion (Luedtke, 2004). The turbine’s rotor is connected to a LP compressor’s one by a coupling, the same way as the compressors’ rotors are connected to each

other. The LP and MP casings have nine stages each whereas the HP unit stage number is seven. The HP casing is also equipped with a single recirculation stage.

Initially, the compressor was built in order to supply one of the circuits utilized in ammonia production. The role of the recirculation stage was to provide the flow through the circuit whereas the task of the compression module was to keep the pressure within the circuit at a constant level. Due to technological aspects the chemical compositions of the gaseous mixtures flowing through the compression module and through the recirculation stage differed: the medium consisting mainly of hydrogen (74%) and nitrogen with small amounts of methane and argon was compressed within the compressor while the ingredients of recirculation stage's operating mixture also included $NH_3$. Obviously, the design mass flows of the compression module and of the recirculation stage also differed. The precise values of the latter as well as of the other nominal operating parameters of each compression unit are listed in Tab. 1.

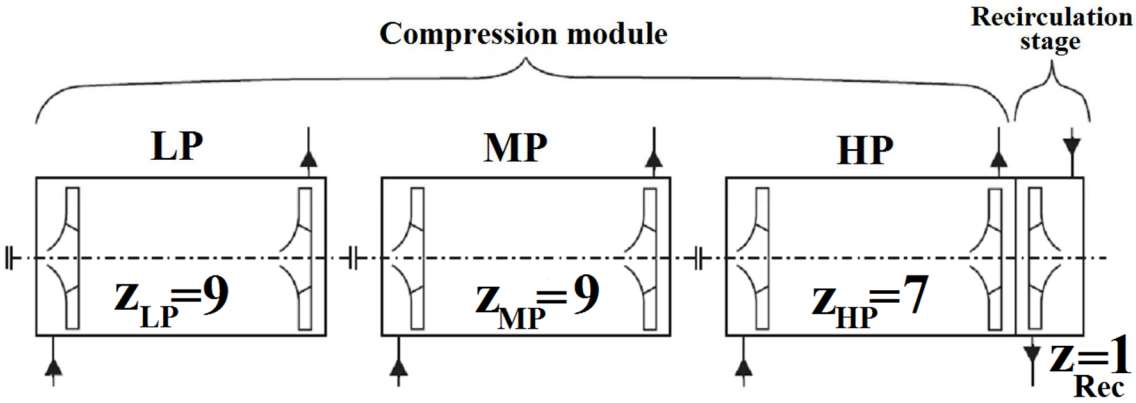


Figure 1: **Scheme of conventional compressor configuration**

Table 1: **Operating conditions of conventional compressor at design point**

| Parameter | LP | MP | HP | Rec |
|---|---|---|---|---|
| $p_{in} \cdot 10^{-5}$, Pa | 24.5 | 70.3 | 137.9 | 202.6 |
| $p_{out} \cdot 10^{-5}$, Pa | 71.1 | 139.3 | 210.9 | 218.8 |
| $T_{in}$, K | 305 | 306 | 306 | 299 |
| $T_{out}$, K | 468 | 412 | 375 | 307 |
| $\dot{m}$, kg/s | 9.521 | 9.521 | 9.521 | 61.170 |
| $\Pi_{in-out}$ | 2.90 | 1.98 | 1.53 | 1.08 |
| $\eta_p$ | 0.629 | 0.605 | 0.585 | 0.674 |

Fig. 2 illustrates the meridional cross-section of the first seven stages of the MP module. The impellers of the first six stages are identical with relative outlet width of $b_2 / D_2 = 0.02$, hub ratio of $\nu = 0.3$ and outlet blade angle of $\beta_{bl2} = 36°$. The specific flow coefficient of the first stage equals to $\Phi_{MP\_I} = 0.011$. Apparently, with gradual increase of flow density throughout the flow path and no alterations done to its geometry the value of $\Phi$ will be steady falling with increase of the stage's number. According to data published in literature the level of achievable efficiency of such an assembly will always lie lower than of a machine where the flow coefficient varies within $0.045 \le \Phi \le 0.055$ (Galerkin, 2010). Indeed, measurements performed at the consumer's facility show that polytropic efficiency $\eta_p$ reached by MP compressor at design point is no higher than 61% (see Tab. 1). Even though the unit was equipped with low-solidity vaned diffusers, which according to Dalbert, 1999, are supposed to provide a compromise between higher efficiencies of VD and broader operating ranges of VLD, the energy losses generated mainly by impeller disk friction,

internal flow leakages and positive incidence existing at all stages but the first one did not allow to reach a higher value of $\eta_p$. It seems worth admitting though, that at the time the compressor was manufactured such an efficiency might have been considered even as high assuming that only low flow coefficient machines were taken into account. In a paper by Strizhak (1992) the efficiencies of $0.62 \le \eta_p \le 0.72$ for isolated stages with $0.008 \le \Phi \le 0.012$ are reported what does not lie far away from the machine discussed herein, especially when the losses in inlet and outlet plenums are added.

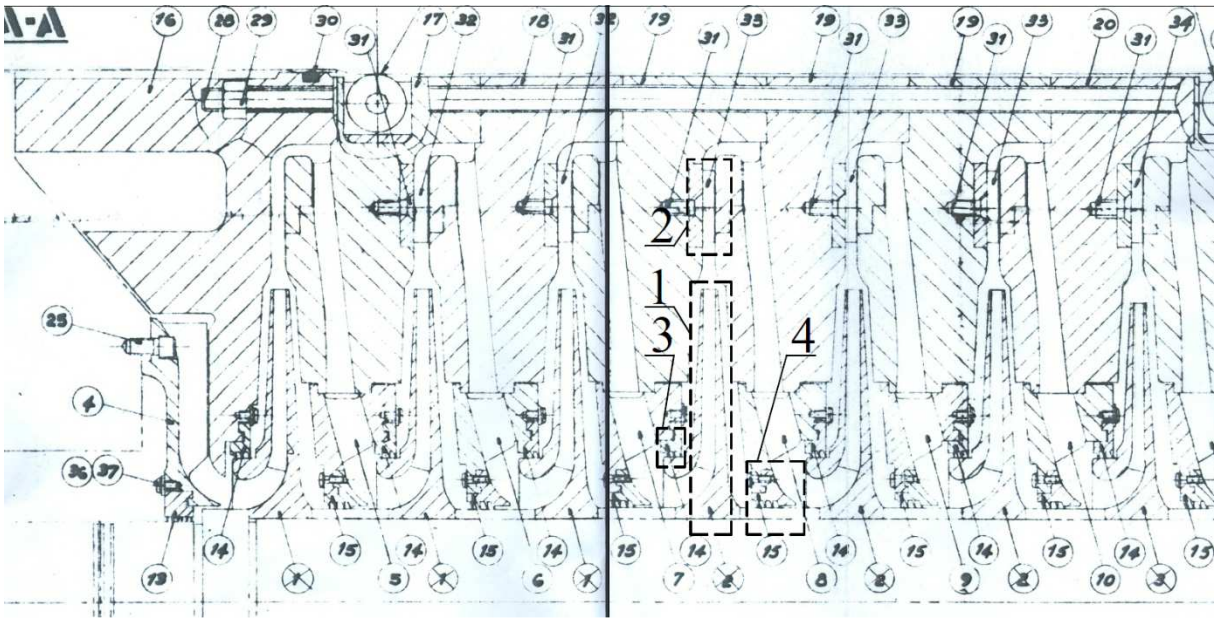


Figure 2: **Meridional cross section of MP module of conventional compressor**

## MODERNIZATION CONCEPTION

### General aspects

The main reason for the modernization of the conventional compressor was the installation of a more efficient converter (one of the main components of the circuit the compressor operated with) that was characterized by a lower pressure drop $\Delta p_{\text{conv}}$. As a result, the discharge pressure $p_{\text{HP\_out}}$ and volumetric flow rate $\dot{V}_{\text{c\_in}}$ required from the compression module shifted to lower values: the relative decrease constituted 33.7% in terms of $p_{\text{HP\_out}}$ and 21.8% in terms of $\dot{V}_{\text{c\_in}}$ (see Tab. 2). The undertaken analyses showed that even with necessary corrections in turbine output, the adaption of the original machine to newer operating conditions would have resulted in an off-design operation and reasonable loss of efficiency. Due to that, the owner of the installation finally announced the revamp of the compression unit which was realized as a common project of Neo-Tec Sp. z O. O. and Institute of Turbomachinery of Lodz University of Technology.

Table 2: **Comparison of several operating parameters of the compression system in its conventional and modernized states**

| | Conventional | Modernized |
|---|---|---|
| $p_{\text{HP\_out}} \cdot 10^{-5}$, Pa | 210.9 | 139.8 |
| $\Delta p_{\text{conv}} \cdot 10^{-5}$, Pa | 16.2 | 9.0 |
| $T_{\text{conv\_in}}$, K | 438 | 413 |
| $\dot{V}_{\text{c\_in}}$, $\text{Nm}^3/\text{s}$ | 122.2 | 95.5 |
| $\dot{V}_{\text{rec\_in}}$, $\text{Nm}^3/\text{s}$ | 27.3 | 24.5 |

The initial step undertaken was reconsideration of the overall stage number of the unit. Due to the decrease of the level of overpressure required by the circuit it came evident that the stage number might be lowered. The number of options of distribution of the stages along the whole module considered for optimization was four and is revealed in Tab. 3.

Table 3: **Variants of compressor configuration considered during modernization**

| Option | LP | MP | HP | Rec |
|---|---|---|---|---|
| A | $z_{LP}=9$ | $z_{MP}=9$ | $z_{HP}=7$ | $z_{rec}=1$ |
| B | $z_{LP}=8$ | $z_{MP}=7$ | $z_{HP}=4$ | $z_{rec}=1$ |
| C | $z_{LP}=9$ | $z_{MP}=9$ | $z_{HP}=0$ | $z_{rec}=1$ |
| D | $z_{LP}=9$ | $z_{MP}=9$ | $z_{HP}=1$ | $z_{rec}=1$ |

The options considered were the following:

- *"A"*. The number of stages is left the same as in the original machine. The impellers' geometry (mainly blade angles) is however changed in order to satisfy newer operating conditions. This option benefits from almost lack of any necessity to introduce design changes into the outer barrel casings and lubrication and cooling systems and saves manufacturing costs. On the other hand, such an approach will lead to undesirably high energy losses due to disk friction and flow leakages as the number of stages is then too high for the specified pressure ratio.
- *"B"*. The accumulated number of stages is reduced to 19. The stage number distribution and impellers' geometry are optimized in order to reach the highest estimated level of efficiency possible. These alterations lead to reasonable changes in rotor dynamics which have to be taken into account by re-estimating the critical speeds as well as the levels of mechanical vibrations. The intercoolers and oil-system might be left unaltered, though.
- *"C"*. Only two of three casings are used for compression. The overall friction surface and flow leakage are minimal what implies the estimated rates of efficiency to be the highest out of four options considered. However, the fact of employing the "blind" rotor in the HP module with only recirculating impeller mounted results in a need for compensation of additional axial force. Moreover, the heat generated by friction between the shaft's surfaces and the surrounding gas will require the employment of auxiliary convective cooling system in order to keep the temperature of HP casing at a considerable level.
- *"D"*. The option differs from the previous one by supplying the HP casing with a single stage to compensate the axial load on the recirculation stage. The problem of high friction heat emissions still stays, though.

After several discussions held between the owner and the team responsible for modernization the compromising "B" option was chosen for further development.

**Technological aspects**

The major technological change concerned the method of manufacturing the impellers. In conventional unit, the shroud disks were connected with the main ones by means of welding. In modernized compressor it was decided to launch the blades with the cover utilizing high-temperature brazing. One of the main advantages of this method against welding is that the protective atmosphere (inert gas, vacuum etc.) within the furnace allows for better material properties possessed by the final product (Boughton and Roberts, 1973).

The rest of the parts (shafts, couplings, casing diaphragms etc.) did not undergo any crucial technological alteration.

**Design aspects**

The first aspect to be mentioned is the increase of the axial stage pitch resulted from the lower number of stages employed in each casing. According to research published by Lindner (1983) and Galerkin (2010) such a change should have a positive effect on stage performance due to more uniform distributions of meridional velocity at the impellers' inlets.

Considering the alterations of impellers' design, major attention was paid to the search of the optimal values of blade angles and blade numbers. Minor attention was paid to variation of impellers' diameters and heights at inlet and outlet due to spacious limitations. The brief comparison of geometric parameters of conventional and modernized wheels is presented in Tab. 4.

Table 4: **Comparison of geometric parameters of conventional and modernized impellers**

| Module | | LP | MP | HP |
|---|---|---|---|---|
| Outlet blade angle $\beta_{bl2}$,° | Conventional | 45.5 – 30.0 | 36.0 – 36.0 | 30.0 – 30.0 |
| | Modernized | 42.0 – 30.0 | 42.0 – 32.0 | 28.0 – 29.0 |
| Blade number, $z$ | Conventional | 13+13 – 11+11 | 11+11 | 11 |
| | Modernized | 13+13 – 11+11 | 11+11 | 13 |

The lower value of overpressure required from the modernized machine brought to a possibility of application of vaneless diffusers at all of the compression modules. Even though the conventional design implied the use of vaned diffusers with low solidity (or with a reduced chord length) it happened that the diffuser assemblies tended to be a source of additional dynamic stresses due to blade vibrations. It was suggested therefore that the employment of VLD should help to eliminate this undesirable trend.

The last aspect concerned the re-design of labyrinth seals. As all of the stages possessed considerably low design flow coefficients any modification done in order to reduce the labyrinth leakages should have brought to a tangible improvement in stages' efficiency. Due to that it was decided to introduce two major alterations:

- firstly, to minimize the labyrinth radial gap by employing the abradable seals;
- secondly, to manufacture the labyrinths on rotating parts of assemblies (impellers' shrouds and distance sleeves).

According to research by Casey (1990) the second modification might be especially useful in case of high-pressure barrel compressors.

The alterations described above were accepted not only on the basis of mathematical or numerical modelling. Besides of applying the codes developed at IT TUL several pieces of experimental research have been done in order to test the performance of the re-designed stages. The following sections reveal the details of such a test undertaken in terms of the fourth stage of MP module and also report some results of the CFD modelling of its performance.

## TEST BENCH FOR VERIFICATION OF DESIGN CALCULATIONS

The scheme of meridional outline of the test rig is shown in Fig. 3.a. The unit has been developed at the IT TUL in 1997. According to the scheme the stand's flowpath consisted of three basic parts: *inlet duct* equipped with a circular inlet pipe (pos. 1), an orifice for mass flow measurements (pos. 2) and a circular plenum (pos. 3); *compression stage* consisting of a radial IGV assembly (pos. 4), an impeller wheel (pos. 5) and a vaneless diffuser (pos. 6); *outlet duct* including a discharge chamber (pos. 7) and an outlet pipeline. The impeller was fitted on a shaft (pos. II) supported by a pair of ball bearings (pos. I) and connected to the electric drive (pos. V) via a coupling system (pos. III) and a two-stage multiplying gearbox (pos. IV). The design allowed the impeller to rotate at a tip speed of $u_2 = 230\,\mathrm{m/s}$ what at normalized inlet conditions ( $p_{in}^{*} = 101325\ \mathrm{Pa}$ , $T_{in}^{*} = 288\,\mathrm{K}$ ) brought to the tip

Mach number of $M_u = 0.68$. The main geometric parameters of the impeller as well as of VLD are listed in Tab. 5.

Table 5: **Main geometric parameters of test impeller and VLD**

| $D_2$, mm | $D_h / D_2$ | $D_0 / D_2$ | $D_4 / D_2$ | $b_2 / D_2$ | $b_4 / b_2$ | $\beta_{bl2}$ ° | $z$ |
|---|---|---|---|---|---|---|---|
| 425 | 0.3 | 0.4 | 1.39 | 0.02 | 0.97 | 36 | 11+11 |

The data acquisition system used during the measurements included static pressure taps, total pressure tubes and thermocouples located at corresponding control sections that are also marked in Fig. 3.a. The parameters measured included mainly pressures (static $p$ and total $p^*$) and temperatures (static $T$ and total $T^*$). The most "loaded" sections were *0'-0'* and *4'-4'* where the measured parameters set included $p$, $p^*$ and $T^*$. Pressure signals were collected by Scanivalve scanner whereas temperature signals – by Keythley temperature measurement system. Both devices sent the received data to the PC where they were processed and stored.

a

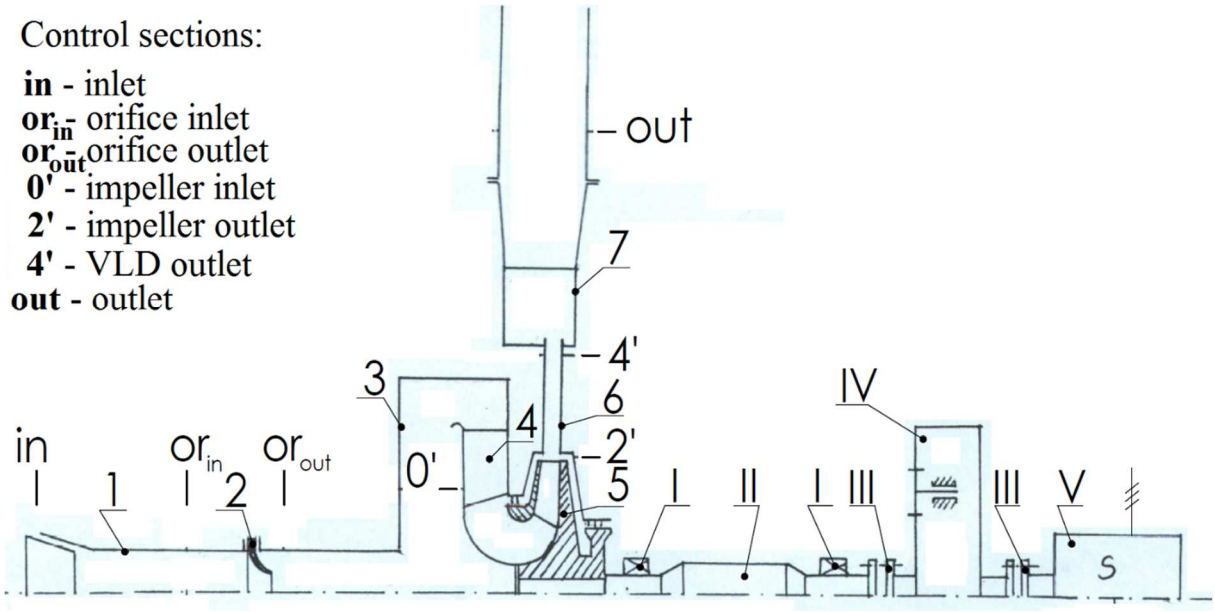


b

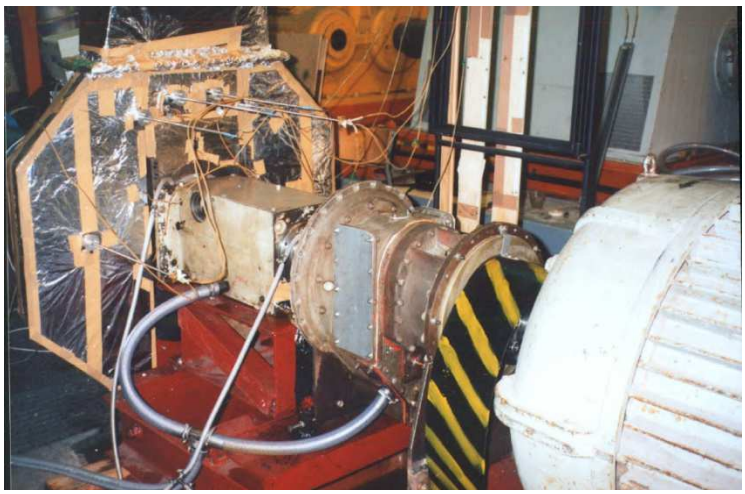

c

Figure 3: **Scheme of test rig meridional cross-section (a), rear view of the test rig (b), front view of the test rig (c)**

## NUMERICAL MODEL OF THE TEST STAGE

The computational domain shown in Fig. 4.a was developed using various CAD software on the basis of geometrical data from internal materials of IT TUL. Due to the expected tangible impact of the disk friction and labyrinth leakages on the stage performance it was decided to include the corresponding channels (pos. 4, 5) into the domain's contents, which besides of the ones also possessed the inlet (pos. 1), impeller (pos. 2) and VLD (pos. 3) channels.

All the sub-domains but the impeller's one were modelled as stationary. The impeller was given the rotational speed of $n = 10340\text{rpm}$. In order to reduce the time duration of a single simulation the flow was assumed to be modelled as time-steady and circumferentially periodic. Therefore, only two blade passages (main and splitter) were considered. The $k-\omega$ SST turbulence model by Menter, 1993, was applied whereas the convective fluxes were discretized with the "high-resolution" scheme. Commercial Ansys CFX 16.2 code was chosen as a computational environment.

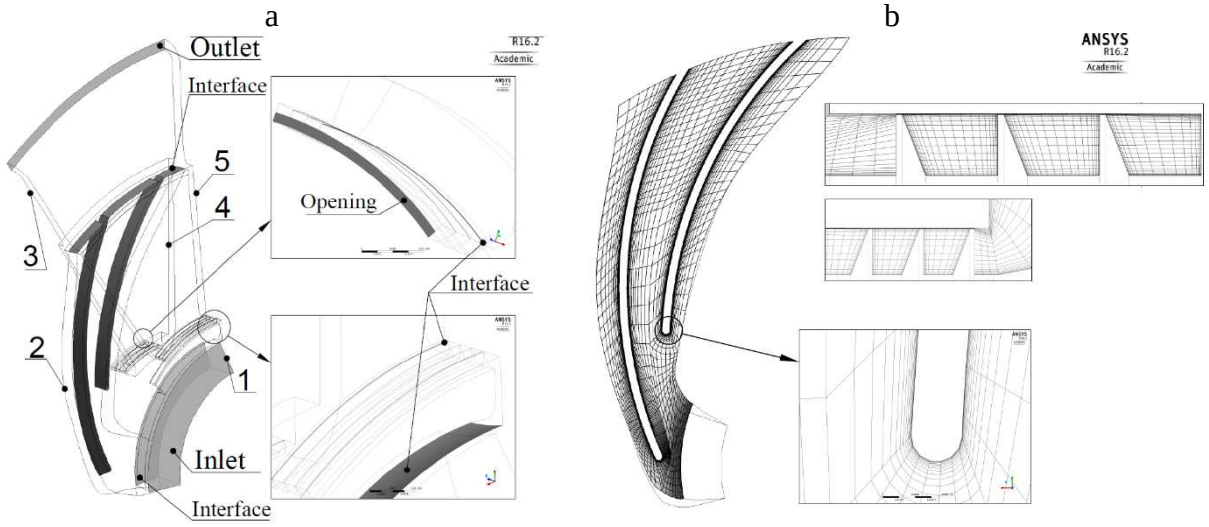


Figure 4: **Isometric view of the computational domain (a) and samples of the computational grid (b)**

Table 6: **Maximal values of y+ on the wall surfaces**

| Domain | Hub | Shroud | Main blade | Splitter blade |
|---|---|---|---|---|
| Impeller | 102 | 102 | 47.7 | 13.6 |
| VLD | 16.1 | 16.4 | – | – |
| Lab. seal hub | 9 | 7 | – | – |
| Lab. seal shrd | 9 | 8 | – | – |

The finite volume grid used in the computations (see Fig. 4.b) was built in ICEM CFD 16.2 and consisted of 393000 hexahedrons. The impeller mesh was created in a way to possess two C-grid blocks around each of the blades, the rest of the mesh was built as an H-grid.

At the inlet boundary the total pressure $p_{\text{in}}^{*} = 101325$ Pa, total temperature $T_{\text{in}}^{*} = 288\ K$, turbulence intensity $Tu = 5\%$ and eddy viscosity ratio $\mu_{\text{T}} / \mu = 10$ were specified and were kept the same for every operating point simulated. At the outlet boundary, however, the parameter specified depended on the operational regime: integrally averaged static pressure $p_{\text{out\_ave}}$ was set for the range $\Phi_{\text{d}} = 0.012 \le \Phi \le \Phi_{\max}$ and mass flow rate $\dot{m}_{\text{out}}$ for $\Phi < \Phi_{\text{d}}$. Opening BC was specified on the surface supposed to connect the last of the shaft's labyrinth chambers with the inlet of the following stage. Opening total temperature $T_{\text{op}}^{*}$ and static pressure $p_{\text{op}}$ were set to equal to the values at the

outlet boundary. The flow velocity on the wall surfaces was specified to be zero ("no-slip" boundary condition) whereas the very walls were treated as adiabatic ones. Walls reproducing impeller's or shaft's surfaces were rotating with the same speed as the impeller. All the domain's interfaces operated using the approach known as "stage" in Ansys CFX.

## RESULTS OF EXPERIMENTAL MEASUREMENTS AND NUMERICAL MODELLING OF TEST STAGE PERFORMANCE

The main results obtained during the tests and numerical simulations are illustrated in Fig. 5 in terms of dependences of stage pressure ratio $\pi_{0'-4'}$ and total isentropic efficiency $\eta^*_{s\_0'-4'}$ on specific flow coefficient $\Phi$.

Comparing the experimental pressure rise curve to the computed one it is visible that the acceptable level of results coincidence is only achieved at design point ($\Phi_d = 0.012$). At off-design operation the model either underpredicts the outlet pressure ($\Phi < \Phi_d$) or overpredicts the flow rate ($\Phi > \Phi_d$). In order to interpret this trend it is worth applying to the relation which could be derived from a one-dimensional form of Bernoulli equation (Galerkin, 2010):

$$\pi_{i-j} = \left(1 + (k-1)\Psi_T M_u^2\right)^{\frac{k\eta_{p\_i-j}}{k-1}}. \qquad (1)$$

Out of 1D Euler equation for turbomachinery assuming the condition of zero inlet flow pre-swirl $c_{u1} = 0$ and the definition of velocity triangle at impeller outlet as in the Figure 5,c the theoretic head coefficient may be written as $\Psi_T = \frac{c_{u2}}{u_2}$. With $k, M_u = idem$ it occurs that the observed deviation between the measurements and NS should be caused by errors in prediction of $c_{u2}$ and polytropic efficiency $\eta_{p0'-4'}$. However, the evaluation of quantitative contribution of each factor into the resulting error was not possible in terms of this work as the measurements of the flow direction at impeller outlet were out of scope of the experimental tests.

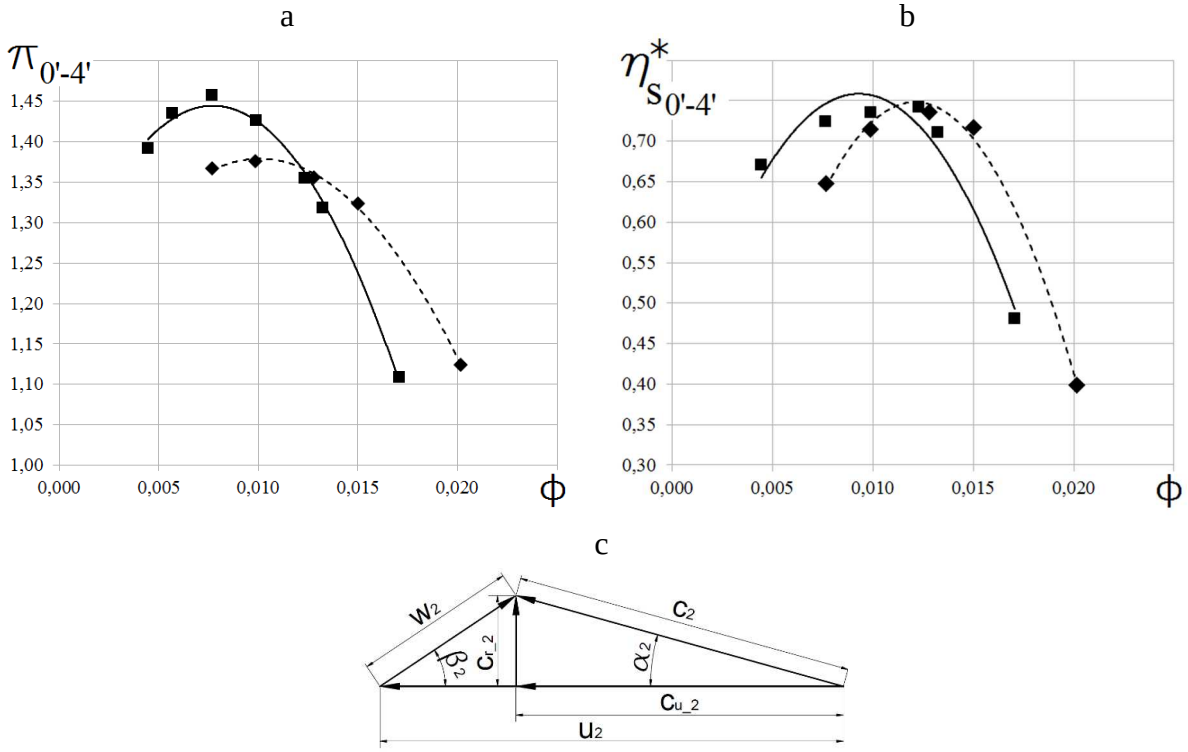


Figure 5: **Experimental (solid line) and computed (dashed line) dependences of the stage pressure ratio $\pi_{0'-4'}$ (a), isentropic efficiency $\eta^*_{s\_0'-4'}$ (b) and a schematized velocity triangle at impeller outlet (c)**

Looking at isentropic efficiency maps shown in Fig. 5.b it might be observed that the trend of marginal shifting of the numerical curve to the right hand side of the map stays present. The curves look similarly to each other from the qualitative viewpoint, but the quantitative level of coincidence is still not high. The only exception from the trend is again the design point where the numerically and experimentally obtained values of $\eta^*_{s\_0'-4'}$ are almost identical. As was mentioned above, the reason for the discrepancy existence may be identified only after additional series of tests or after modifications done to the model, which is left as a subject for further works. Beyond the CFD-experiment comparative analysis it is important to state that the level of the maximal efficiency achieved is very close to 75%, which is quite high for a low flow coefficient stage with VLD (Dalbert, 1999).

Since the satisfactory level of numerical simulations accuracy was only reached at the design point and due to the bounded size of a single publication it was decided to pay a deeper attention to the analysis of flow pattern modelled only at that operating condition. As one of the major modifications done to the design of the modernized machine was a shift to vaneless version of radial diffusers keeping the same diffuser diameter ratio, the main goal was to see how efficient will be the operation of VLD at the existing design constraints.

Fig. 6 shows the distributions of circumferential $c_u$ (a) and radial $c_r$ (b) velocities and of the flow angle $\alpha$ (c) along the diffuser height as well as velocity triangles based on integrally-averaged values of velocities respectively at diffuser inlet ($D_{VLD\_in}/D_2 = 1.08$), middle ($D_{VLD\_middle}/D_2 = 1.20$) and outlet ($D_{VLD\_out}/D_2 = 1.37$).

The circumferential velocity distributions do not identify the existence of any undesirable flow feature as e. g. a stall cell along the whole diffuser radial length. The gradual decrease of $c_u$ in the mainstream with the increase of radius should outcome from the existence of the free-vortex flow. The curves of the radial velocity, however, look less optimistic. Due to the appearance of a moderate backflow zone close to the shroud wall at diffuser middle the whole velocity profile at that location is skewed what finally results in a relatively low overall flow deceleration in radial direction ($c_{r\_VLD\_out}/c_{r\_VLD\_in} = 0.84$). Due to the same reason the axial distribution of the flow angle at VLD outlet gets less uniform than at its inlet. In a real compressor these under-deceleration and non-uniformity will most probably result in higher losses in the return channel due to higher friction and incidence (Galerkin, 2008). However, it was decided to stick to the design with VLD rather to go for VD due to the existed issues with VD vanes vibrations mentioned above.

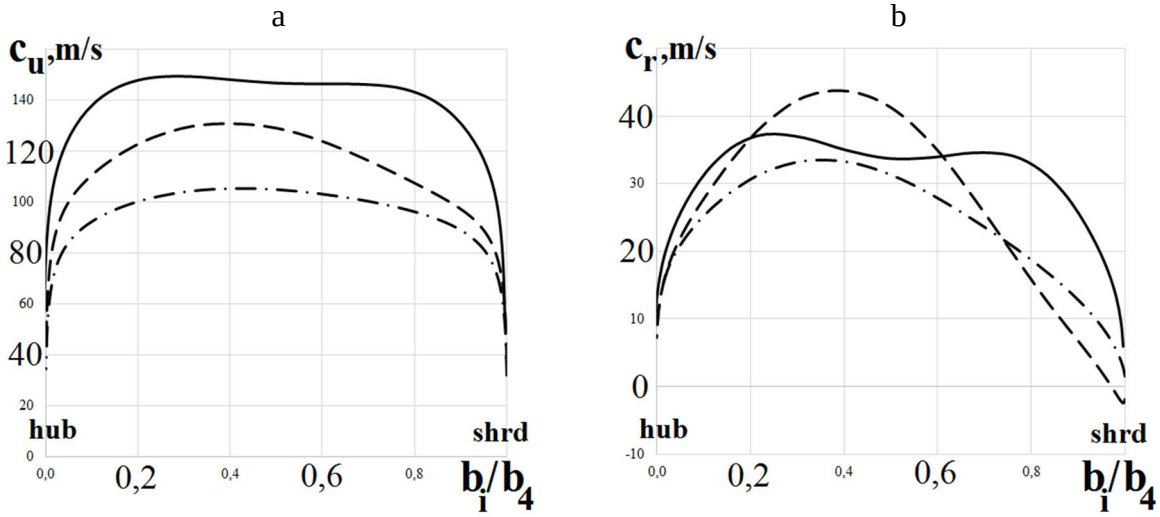

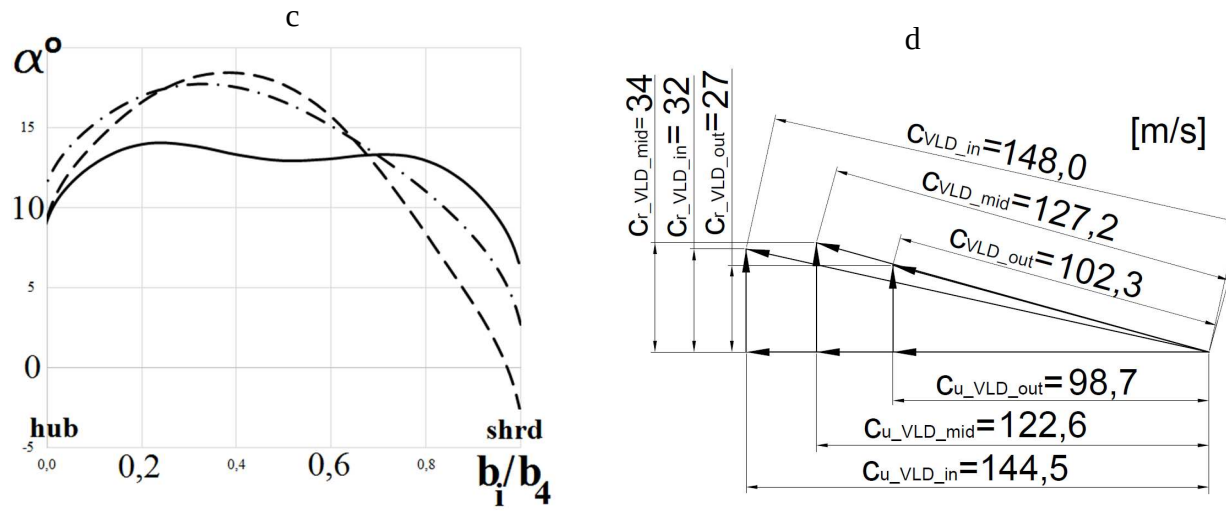


Figure 6: **Dependences of circumferential $c_u$ (a) and radial $c_r$ (b) velocities, flow angle $\alpha$ (c) on dimensionless diffuser height $b_i / b_4$ and velocity triangles at VLD inlet, middle and outlet (d): solid line – VLD inlet, dashed line – VLD middle, dash-dotted line – VLD outlet**

## RESULTS OF START-UP TESTS OF MODERNIZED MACHINE

Due to the design changes introduced the final product of the revamp actually represented a new machine as all the rotors' parts and the internal casings were manufactured from fresh blanks. The MP module assembly of a modernized compressor is illustrated in Fig. 7. The fourth stage, which has been the main subject of the previous section, is marked as "MP4".


Figure 7: **MP rotors of a modernized compressor and HP rotor during assembling**

The results of the measurements of the modernized compressor pressure ratio and volumetric flow rate performed during the start-up tests are shown in Fig. 8. The locations of the required operating point (*"Req. OP"*) and of the parameters measured (*"Real OP"*) almost coincide. The relative deviations are 0.1% in terms of pressure and 0.7% in terms of the flow rate. In addition, the operating points of the conventional compressor (*"OP before mod."*) and of the modernized one at 106% load are introduced.

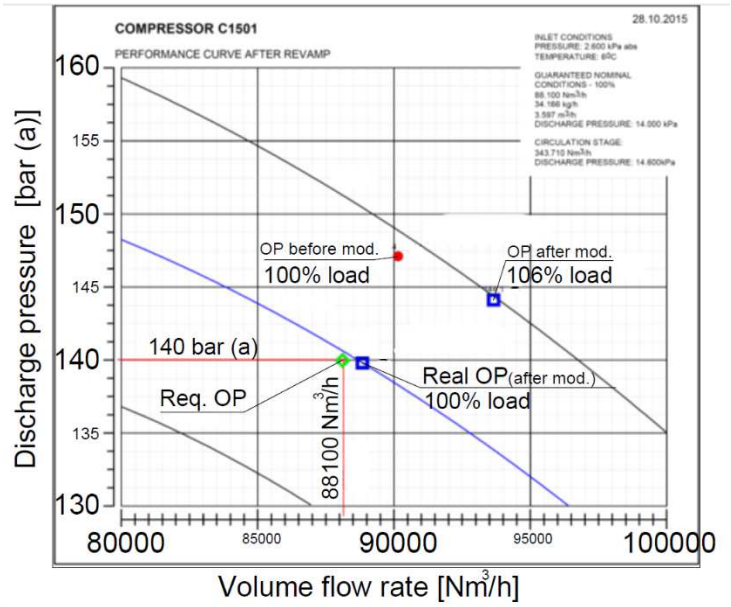


Figure 8: **Results of the start-up performance tests of the modernized compressor**

The measurement data analysis also showed that the polytropic efficiencies of the compression modules improved by 6.2%, 7.5% and 4.5% in terms of LP, MP and HP respectively. The efficiency of the recirculation stage rose by 2.9%.

## CONCLUSIONS

The complex modernization of an industrial multi-hull centrifugal compressor has been undertaken in terms of cooperation between Neo-Tec Sp. z O. O. and IT TUL. The need for the revamp arose due to significant changes in required compressor's output. During the machine redesigning the effort was concentrated on the optimization od impellers' geometry, shifting to VLD instead of LSD and on the introduction of abradable labyrinth seals. Both experimental and computational methods were implemented.

- The CFD modelling of the performance of the fourth stage of MP module showed satisfying conformity with the test data obtained at the corresponding test rig only at design point.
- The analysis of the flow field within 4$^{th}$ MP stage's VLD at design point indicated under-deceleration of the flow in radial direction due to appearance of a small stall region at the shroud wall in the middle part of the diffuser. The diffuser design, however was left unaltered due to mechanical constraints.
- The start-up tests of the modernized compressor showed good correspondence of the machine's output to the required one and indicated overall rise in its polytropic efficiency.

## REFERENCES

Kryłłowicz W., Jóźwik K., Magiera R., (2007), *Selected problems of modernizations of fans and radial compressors*, 7$^{th}$ Conference of Power Engineering, Thermodynamics and Fluid Flow – ES 2007, Pilsen, Czech Republic

Kryłłowicz W., Klonowicz W., Matyjewski M., Kaszak A., (2007), *Wet and dry compression of soda gas: comparison of the industrial turbocompressor performances*, VII-th European Conference on Turbomachinery, Athens, Conference Proceedings, pp. 553 – 564

Kryłłowicz W., Kozanecki Z., Świder P., (2011), *Modernization of a nitrous gas turbine-driven turbocompressor*, Mechanics and Mechanical Engineering, 15, pp. 289 – 296

Kryłłowicz W., (2013), Theory and practice of the centrifugal compressors modernization, Publishing House of Lodz University of Technology, ISBN 978-83-7283-531-4, (in Polish), Łódź

Kozanecki Z. (2008), Rotating Systems of the Low and Medium Power Turbomachinery, ITE Publishing House, ISBN 978-83-7204-693-2, (in Polish), Łódź-Radom

Luedtke K. H., (2004), Process centrifugal compressors, Springer Verlag Heidelberg Berlin, Berlin

Galerkin Y.B., (2010), Turbo compressors, KHT, Moscow (in Russian)

Dalbert P., Ribi B., Kmecl T., Casey M.V., (1999), *Radial compressor design for industrial compressors*, Proc. IMechE Part. C, 213, pp. 71 – 83

Strizhak L. Ya., (1992), *Improvement in the flow-through part of high-pressure centrifugal compressors*, Chemical and Petroleum Engineering, 28, pp. 85 – 91

Boughton J. D., Roberts P. M., (1973), *Furnace brazing: a survey of modern processes and plant,* Welding and metal fabrication

Lindner P., (1983) *Aerodynamic tests on centrifugal process compressors – influence of diffuser diameter ratio, axial stage pitch and impeller cutback,* ASME Journal of Engineering for Power, 105, pp. 910 – 919

Casey M. V., Dalbert P., Schurter E., (1990), *Radial compressor stages fort low flow coefficients*, Presented at the 4th European Congress on Fluid Machinery for Oil, Petrochemical and Related Industries, The Hague, The Netherlands, Imech Paper C403/004

Menter, F.R., (1993), *Zonal two-equation k-ω turbulence model for aerodynamic flows*, AIAA Paper 1993-2906